On the Total Synthesis of Archaeal and Mycobacterial Natural Products

Holzheimer, Mira

DOI:
10.33612/diss.150711132

CHAPTER 4

Synthesis of the Tricyclic Biphytanediol of Crenarchaeol and Structure Revision of Crenarchaeol

This chapter describes the synthesis of the proposed structure of the tricyclic biphytanediol part of crenarchaeol, the comparison with natural crenarchaeol by means of GC-MS and NMR, and the structure revision of naturally occurring crenarchaeol. The work described in this chapter contains contributions from Prof. Stefan Schouten and Prof. Jaap S. Sinninghe Damsté, NIOZ Royal Netherlands Institute for Sea Research.

Completion of the synthesis of the tricyclic biphytanediol of crenarchaeol

Synthesis

Dithiane alkylation

With the synthesis of the Western and Eastern Fragment required for the construction of the target biphytanediol **1** completed, the coupling of both Fragments by dithiane alkylation was investigated.

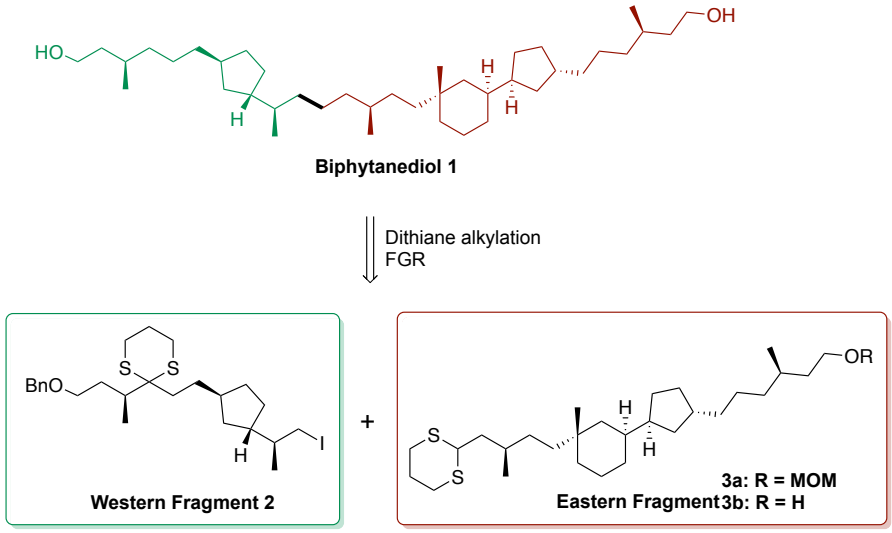

Scheme 1 *Planned construction of biphytanediol* ***1*** *by unification of the Western and Eastern Fragment.*

In order to establish optimal conditions for the dithiane alkylation of iodide **2** with dithiane **3a** or **3b**, first lithiation studies with dithiane **3a** were conducted. For this, **3a** was treated with a strong base at various temperatures, followed by quenching with D_2O and analysis by ^1H NMR (Table 1).

First, lithiation of dithiane **3a** was attempted under the most common conditions for deprotonation (Table 1, entry 1) by treating **3a** with *t*-BuLi in THF/HMPA = 10/1 at -78 ºC. These conditions gave only low levels of lithiation, below 5%. When treating **3a** with *n*-BuLi at 0 ºC or room temperature for up to one hour, only 29% and 24% lithiation was achieved, respectively (Table 1, entries 2 and 3). These results were surprising, as it

was not anticipated that dithiane **3a** would be a difficult substrate for deprotonation. Previous reports using dithiane bearing distal MOM or other acetal-type protecting groups reported good to excellent yields in dithiane alkylations.[1-5] Thus, these results are to date not fully understood.

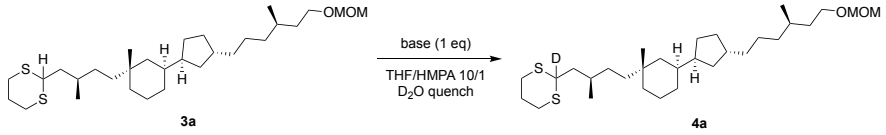

Entry[a]	Base	Temperature	Time	Lithiation
1	*t*-BuLi	-78 ºC	5 min	3%
2	*n*-BuLi	0 ºC	1 h	29%
3	*n*-BuLi	rt	30 min	24%

[a] Determined by ^{1}H NMR by integration and comparison of the signals of the C$\underline{H_2}$OMOM (4.57 ppm, s, 2H) and remaining dithiane CH (4.06 ppm, dd, 1H).

Table 1 *Attempted optimization of lithiation conditions of dithiane* ***3a****.*

Since lithiation of dithiane **3a** proved to be unexpectedly difficult and only a low degree of lithiation could be achieved, lithiation of **3b** – in presence of the free hydroxyl rather than the MOM protecting group – was investigated (Table 2).

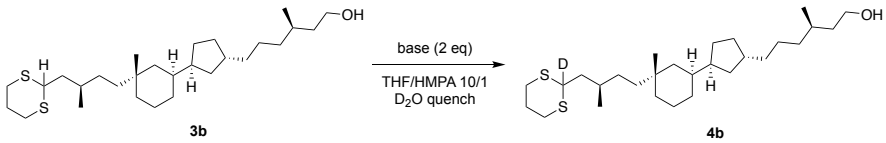

Entry[a]	Base	Temperature	Time	Lithiation
1	*n*-BuLi	0 ºC	30 min	28%
2	*n*-BuLi	-25 ºC	30 min	23%
3	*t*-BuLi	-78 ºC	5 min	71%

[a] Determined by ^{1}H NMR by integration and comparison of the signals of the C$\underline{H_2}$OH (3.55 ppm, m, 2H) and remaining dithiane CH (4.01 ppm, dd, 1H).

Table 2 *Optimization of lithiation conditions of dithiane* ***3b****.*

Treatment of dithiane **3b** with two equivalents of *n*-BuLi in THF/HMPA at 0 ºC and -25 ºC for 30 minutes gave only a poor lithiation efficiency of 28% and 23%, respectively (Table 2, entries 1 and 2). Using *t*-BuLi as base for lithiation of **3b**, however, 71% deuterium incorporation was obtained after five minutes reaction time at -78 ºC (Table 2, entry 3). This result is in sharp contrast to the attempted lithiation of dithiane **3a**, where under the same conditions only 3% lithiation was achieved. This leads to the hypothesis that the MOM ether is attenuating the lithiation of **3a**. However, it is at this point not understood which underlying (electronic) effects cause this drastic difference in lithiation efficiency of **3a** and **3b**.

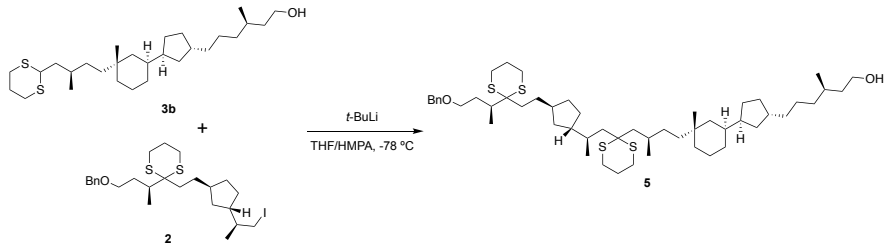

Entry	Dithiane 3b	*t*-BuLi	Lithiation time	Yield[a]
1	1 eq.	2 eq.	5 min	28%[b]
2	1 eq.	2 eq.	10 min	45%[b]
3	1.5 eq.	3 eq.	10 min	67%

[a] Isolated yield. [b] Incomplete conversion of iodide **2**.

Table 3 *Optimization of the dithiane alkylation using iodide **2** and dithiane **3b**.*

After having established suitable lithiation conditions for dithiane **3b**, the dithiane alkylation with iodide **2** was studied (Table 3). Using one molar equivalent of dithiane **3b** (with respect to iodide **2**) and performing lithiation with two equivalents of *t*-BuLi for five minutes gave incomplete conversion of **2** and a low isolated yield of **5** of 28% (Table 3, entry 1). When increasing the lithiation time to 10 minutes, the yield of **5** increased to 45% but again no full conversion of **2** was achieved (Table 3, entry 2). Therefore, dithiane **3b** was taken in slight excess and after lithiation of 10 minutes, the desired coupling product **5** was obtained in good yield of 67% yield (Table 3, entry 3).

Functional group removal – completion of biphytanediol 1

After having completed the assembly of the carbon skeleton of the tricyclic biphytanediol **1** of crenarchaeol, the final step in its synthesis was functional group removal (Scheme 2). For this, as in chapter 2, Raney Nickel desulfurization was chosen. Upon treating **5** with Raney Nickel under an atmosphere of hydrogen at elevated temperature, the dithiane moieties were fully removed, but the benzyl ether partially remained. Thus, the crude product was directly subjected to palladium-catalyzed hydrogenolysis which provided the desired product – biphytanediol **1** – in 42% yield. This unexpectedly low yield was attributed to the difficult purification of **1** by flash chromatography.

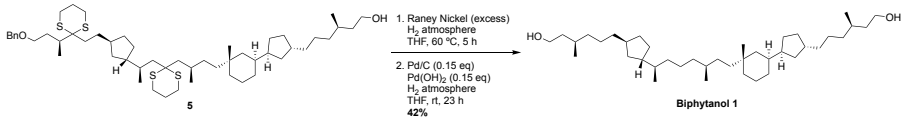

Scheme 2 *Functional group removal of **5** concluded the synthesis of biphytanediol **1**.*

The asymmetric synthesis of biphytanediol **1**, starting from pimelic acid, was completed in 27 steps in the longest linear sequence.

Comparison of the synthetic biphytanediol with natural crenarchaeol

Chemical derivatization and GC-MS analysis

With the synthesis of biphytanediol **1** completed, we set out to investigate if the proposed structure and stereochemistry of the natural tricyclic biphytane matches the synthetic material. In order to allow for direct comparison of synthetic and natural material, first both – a sample of natural crenarchaeol and synthetic diol **1** – were converted to their corresponding hydrocarbons.[6] This was done by treatment of either **1** or crenarchaeol with concentrated HI to give the corresponding primary iodides, which were subsequently reduced to the hydrocarbons with PtO_2 (Fig. 1A). The chemical derivatization of crenarchaeol (a mixture of crenarchaeol and crenarchaeol isomer) provided a mixture of bi- and tricyclic biphytanes **BPI**, **BPII** and **BPIII**, whereas derivatization of **1** gave a single biphytane **BPIV**.

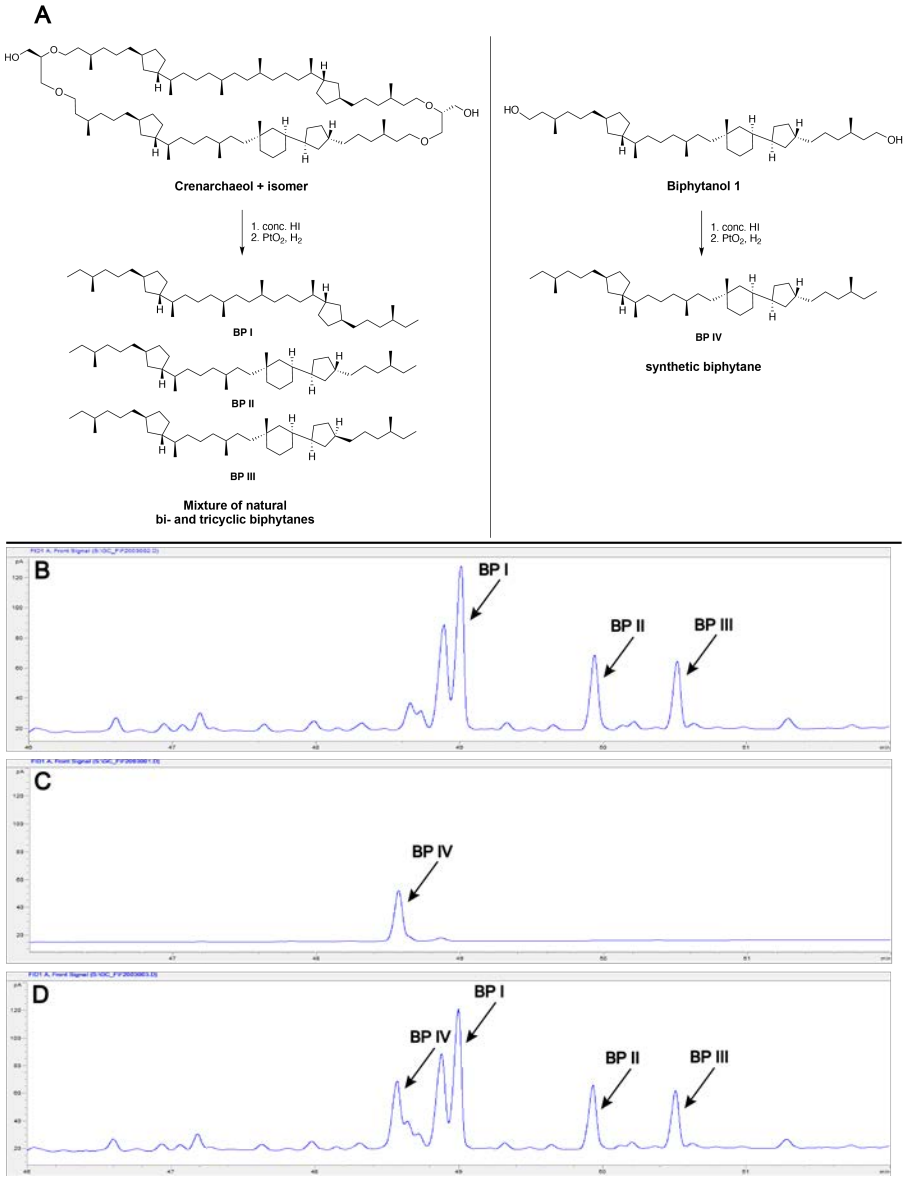

Fig. 1 A: *Chemical derivatization of natural crenarchaeol and synthetic biphytanediol* ***1*** *to the corresponding biphytyanes* ***BP I-IV*** *allows for direct comparison by GC-MS.* ***B:*** *Partial gas chromatogram of natural biphytanes* ***BP I-III*** *from the GDGTs in the Bligh Dyer extract of the thermophilic Thaumarchaeota "Ca. Nitrosotenuis uzonensis".*[6] ***C:*** *Partial gas chromatogram of synthetic biphytane* ***BP IV*** *generated from synthetic biphytanediol* ***1****.* ***D:*** *Co-injection of natural and synthetic biphytanes.*

The natural and synthetic biphytanes were analysed by GC-MS. The derivatization products derived from the GDGTs in the Bligh Dyer extract of the thermophilic Thaumarchaeota ‘‘Ca. Nitrosotenuis uzonensis”, which are dominated by crenarchaeol and its isomer,[6] appeared in a ratio of approximately 1:1 bicyclic to tricyclic biphytanes (Fig. 1B).

The synthetic biphytane **BP IV** appeared as single peak in the chromatogram, confirming the presence of a single stereoisomer (Fig. 1C), *albeit with a different retention time than **BP II** in the natural sample.* Co-injection of natural and synthetic biphytane products ultimately confirmed the mismatch between (synthetic) **BP IV** and (natural-derived) **BP II**. This was evident by a significant difference in retention time between **BP IV** of around 1.5 min and 2 min compared to **BP II** and **BP III**, respectively (Fig. 1D). After scrutinizing all synthetic steps in the synthesis of **1**, and re-analyzing the characterization of all intermediates, this single GC-MS trace led to the conclusion that the structure of the tricyclic biphytane of natural crenarchaeol, and therefore the structure of crenarchaeol itself, had to be revised!

Next, the mass spectra of the biphytanes **BP I**-**IV** were analysed (Fig 2). The fragmentation patterns of **BP I-III** were in good agreement with previously reported mass spectral analysis.[6, 7] The mass spectrum of bicyclic **BP I** featured diagnostic fragments of *m*/*z* 390 and *m*/*z* 362. Both the two natural tricyclic **BP II** and **BP III** as well as synthetic **BP IV** showed the characteristic fragment *m*/*z* 262, attributed to the bond cleavage adjacent to the quaternary stereocenter. Interestingly, the mass fragments of **BP II** and synthetic **BP IV** are virtually identical, including the characteristic *m*/*z* 262/263 ions,[6, 7] indicating that the overall chemical connectivity of **BP II** and **BP IV** is the same. Thus, we hypothesized that **BP II** and **BP IV** are stereoisomers of each other.

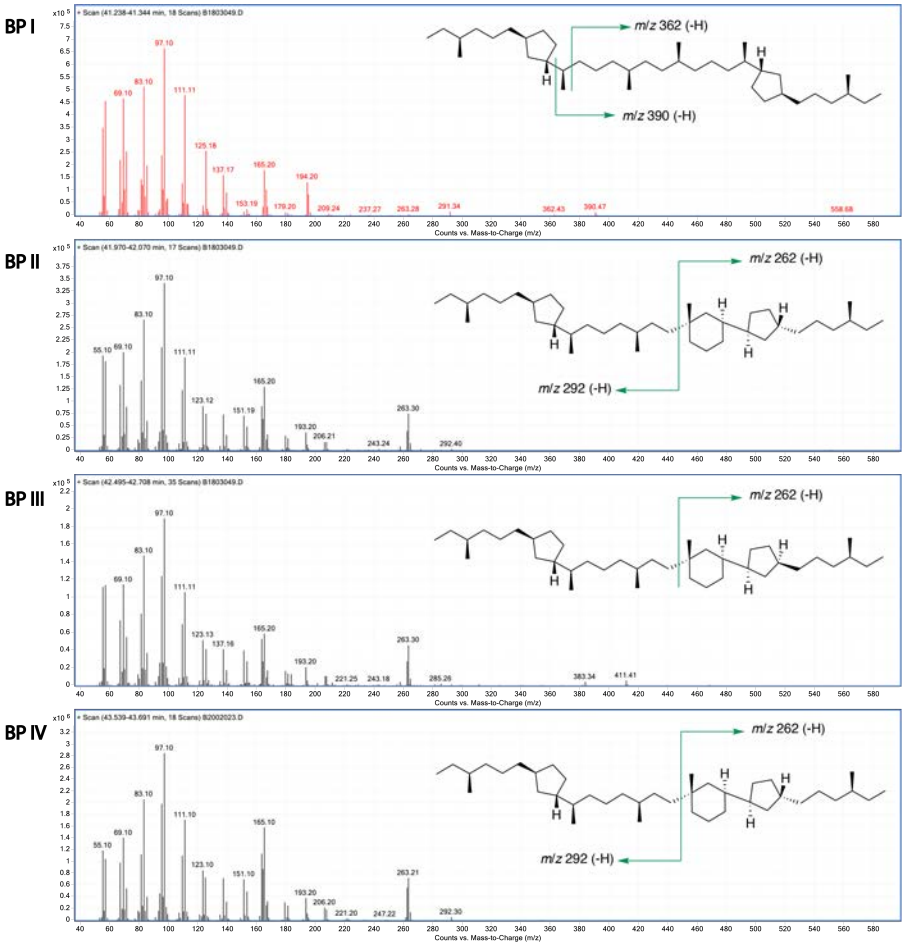

Fig. 2 *Mass spectra (70 eV) of natural biphytanes* ***BP I-III*** *and synthetic* ***BP IV*** *with characteristic fragment ions indicated.*

NMR analysis of biphytanediol 1 and comparison with crenarchaeol

In order to gain further insight into the exact difference between synthetic biphytanediol **1** and the tricyclic biphytane of crenarchaeol, the NMR spectra of **1** and crenarchaeol were compared. Assignment of the ^{1}H and ^{13}C signals of crenarchaeol[8] and **1** was done by extensive 2D NMR analysis (^{1}H-^{13}C HSQC, ^{1}H-^{13}C HMBC, ^{1}H-^{1}H COSY and ^{1}H-^{1}H NOESY). Comparison of the ^{13}C NMR shifts of crenarchaeol and **1** are shown in Table 4. Numbering of

the carbons is shown in Fig. 3 and significant ^{13}C NMR shift differences of **1** relative to crenarchaeol are highlighted in red and orange.

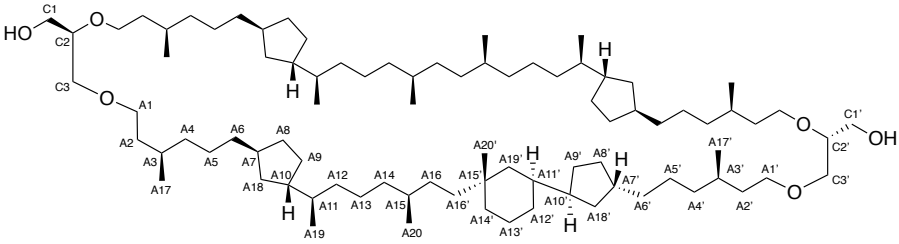

crenarchaeol

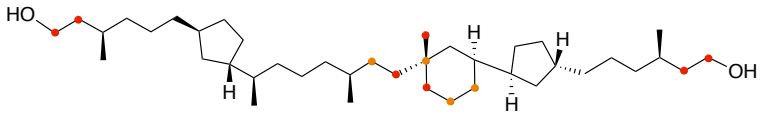

synthetic biphytanol 1

Fig. 3 *Proposed structure of crenarchaeol with numbering of the carbon atoms in the tricyclic biphytane chain and the glycerol backbone.[8] The bicyclic biphytane chain of crenarchaeol is numbered from B1 to B20 in analogy to the tricyclic biphytane (not shown in the structure). Some carbon atoms in synthetic biphytanediol **1** represent moderately ($\Delta\delta$ 0.25–1 ppm, orange) and strongly ($\Delta\delta$ >1 ppm, red) shifted ^{13}C NMR signals compared to those of crenarchaeol.*

Carbon number	^{13}C crenarchaeol (ppm)	^{13}C diol 1 (ppm)	Δδ ^{13}C (ppm)
A1, A1'	70.23, 70.26	61.42	-8.81, -8.84
B1, B1'	68.72 (2x)	–	–
A2, A2'	36.72, 36.75	40.14, 40.15	+3.42, +3.40
B2, B2'	37.18 (2x)	–	–
A3, A3', B3, B3'	29.84, 29.85, 29.92, 29.93	29.63, 29.65	-0.21, -0.21
A4, A4', B4, B4'	37.34, 37.37, 37.42, 37.45	37.52, 37.55	max. -0.21
A5, A5', B5, B5'	26.00 (3x), 26.04	26.05	+0.01, +0.05
A6, A6', B6, B6'	37.28, 37.29 (2x), 37.30	37.31, 37.40	+0.03, +0.10
A7, B7, B7'	39.25, 39.23 (2x)	39.24	-0.01
A7'	39.00	39.00	±0.00
A8, B8, B8'	33.52 (3x)	33.39	-0.13
A8'	33.47	33.36	-0.11
A9, A9', B9, B9'	31.36, 31.40, 31.33, 31.34	31.34, 31.41	-0.02, +0.01
A10, B10, B10'	44.92, 44.88, 44.89	44.96	+0.04
A10'	45.82	45.73	-0.09
A11, B11, B11'	38.36, 38.31, 38.33	38.45	+0.09
A11'	39.23	39.01	-0.22
A12, B12, B12'	35.85, 35.81 (2x)	35.87	+0.02
A12'	32.27	31.80	-0.47
A13, B13, B13'	24.56, 24.53 (2x)	24.53	-0.03
A13'	22.40	22.10	-0.30
A14	37.55	37.60	+0.05
A14'	44.13	38.16	-5.97
B14, B14'	37.72 (2x)	–	–
A15	33.70	33.71	+0.01
A15'	33.20	32.92	-0.28
B15, B15'	33.23	–	–
A16	30.12	30.50	+0.38
A16'	37.80	33.51	-4.29
B16, B16'	34.37	–	–
A17, A17', B17, B17'	19.87, 19.91, 19.93, 19.94	19.79	-0.08, -0.12
A18, B18, B18'	36.08, 36.09, 36.17	36.16	-0.01
A18'	36.59	36.61	+0.02
A19, B19, B19'	17.88, 17.79, 17.90	17.90	±0.00
A19'	44.06	43.90	-0.16
A20, B20, B20'	20.10, 20.01 (2x)	20.25	+0.15
A20'	22.55	30.12	+7.57
C1, C1'	63.22	–	–
C2, C2'	78.50, 78.51	–	–
C3, C3'	71.26, 71.28	–	–

Table 4 *Assignments of ^{13}C NMR signals of crenarchaeol and biphytanediol **1**. Spectra of **1** and crenarchaeol were measured in $CDCl_3$ using a Bruker and Varian 600 MHz NMR instrument, respectively. Signals are reported relative to the solvent residual signal (77.16 ppm).*

When the ^{13}C NMR signals of **1** are compared with those of natural crenarchaeol,[8] it becomes evident that the majority of the chemical shifts of **1** correspond well ($\Delta\delta$ < 0.25 ppm) to those of crenarchaeol. In particular, the signals of the Western part (i.e. the isolated cyclopentane ring and its alkyl substituents) are virtually identical. Small differences in chemical shift ($\Delta\delta$ 0.25–1 ppm) were attributed to the ring carbons of the cyclohexane moiety (A12', A13' and A15') as well as on the alkyl chain adjacent to the 6-membered ring (A16). Large chemical shift differences at the (sub)terminal carbons (A1, A1', A2 and A2') of **1** are due to the presence of primary hydroxyl groups contrary to the ether moieties of crenarchaeol. More importantly, three positions around the *all*-carbon quaternary stereocenter show large chemical shift differences, namely positions A14' ($\Delta\delta$ -5.96 ppm), A16' ($\Delta\delta$ -4.29 ppm) and A20' ($\Delta\delta$ +7.57 ppm). Notably, the ^{13}C signals of the remaining stereocenters of the 5-6-ring system (A11', A10' and A7') in **1** are not shifted significantly, indicating that, in these positions, the structure of **1** and the proposed structure of crenarchaeol are congruent. In addition to the good agreement of the ^{13}C NMR chemical shifts of **1** and crenarchaeol, the ^{1}H shifts of A7', A10' and A11' are matching well (Table 5). In A19' (axial) and A20', there are only minor differences. Only the equatorial proton of A19' exhibits a significant ^{1}H shift difference of 0.15 ppm.

Carbon number	^{1}H crenarchaeol (ppm)	^{1}H diol 1 (ppm)
A7'	1.79	1.78
A10'	1.47	1.46
A11'	1.17	1.12
A19'	ax.: 0.70; eq.: 1.39	ax.: 0.64; eq.: 1.52
A20'	0.84	0.79

Table 5 *Comparison of selected ^{1}H NMR signals of biphytanediol **1** and natural crenarchaeol.[8]*

As the relative (and absolute) stereochemistry of **1** are known, the methyl group A20' in **1** is assigned to be in equatorial position as a result of the 1,3-*cis* relationship between the cyclopentyl and the methyl substituents. Due to the deshielding γ-gauche effect, the ^{13}C chemical shift of axial substituents in cyclohexanes is more downfield (i.e. higher ppm) compared to equatorial substituents.[9-12] In biphytanediol **1**, the ^{13}C signal of A20' resonates at 30.12 ppm, whereas in crenarchaeol, the signal of A20' is shifted more upfield

at 22.55 ppm. This data strongly indicates that the methyl substituent A20' of crenarchaeol is axially oriented, contrary to the originally proposed structure[8] (Fig. 3). To further support this hypothesis, we turned our attention to the ^{13}C chemical shifts of A16'. In diol **1**, the first carbon atom of the alkyl side-chain of the cyclohexane moiety (i.e. A16') is in axial position and the ^{13}C signal resonates at 33.51 ppm, while in crenarchaeol the ^{13}C signal of A16' is shifted significantly downfield to 37.80 ppm. Consequently, this downfield shift of A16' in crenarchaeol indicates equatorial substitution of the alkyl chain substituent of the cyclohexane ring, providing additional evidence for an inverted stereochemistry of crenarchaeol at A15' compared to **1**.

Conclusion – Structure revision of natural crenarchaeol

As discussed in Chapter 1, the determination of the structure of crenarchaeol has a considerable history. This is due to the very complex structure, including 22 stereocenters, of the molecule in the first place. The lack of functional groups and rigidity, heavily complicate NMR-based structural studies and as the compound does apparently not have the tendency to crystallize, X-ray diffraction is not possible. To complete the list of hurdles, and despite the fact that crenarchaeol is one of the most abundant marine natural products, its purification from natural sources even in sub-mg amounts is very laborious.

In 2002, Sinninghe Damsté *et al*. proposed the structure of crenarchaeol based on extensive NMR studies and supported by the body of literature on the biosynthesis of the GDGTs.[8] Clearly, at that time already, the structure of the cyclohexyl-linked-to-cyclopentyl ring unit was the most complex, also because this motif is unique in nature. In 2003, Helmchen *et al*. demonstrated – or maybe more correctly – confirmed, by synthesis the identity of the bicyclic biphytane part (the upper part with two cyclopentyl rings, also present in other GDGTs) of crenarchaeol.[13] Somewhat surprizingly, the authors did not refer to the 2002 paper of Sinninghe Damsté but did compare only to natural GDGT-4. Very recently, two reports established the connectivity of the biphytane units to the glycerol backbone.[14, 15]

As part of a first total synthesis of crenarchaeol, we prepared the lower biphythane unit of crenarchaeol. After thorough analysis by chemical

derivatization and subsequent GC-MS analysis as well as NMR comparison of our synthetic biphytanediol **1** with natural crenarchaeol, we can summarize our findings as follows:

- The biphytane product **BP IV** derived from **1** by HI treatment/hydrogenation shows a large difference in retention time (≥ 1.5 min) on GC-MS compared to the tricyclic biphytane product **BP II** derived from crenarchaeol. Therefore, it is concluded that synthetic biphytane **BP IV** is not identical to the tricyclic **BP II** of crenarchaeol.
- The biphytane **BP IV** has an identical mass spectrum as **BP II** of crenarchaeol. Therefore, we conclude the overall chemical connectivity (i.e. carbon skeleton excluding stereochemistry) of **1** and the tricyclic biphytane of crenarchaeol are identical.
- The difference in retention time concomitant with the identical mass spectra strongly indicates a difference in relative stereochemistry.
- Comparison of the ^{13}C NMR shifts reveals significant shift differences around the quaternary stereocenter A15', while the signals of the other stereogenic centers in biphytanediol **1** are virtually identical to those in natural crenarchaeol.
- In **1**, A20' is shifted downfield (30.12 ppm) compared to A20' in crenarchaeol (22.55 ppm), indicating that A20' in crenarchaeol is in an axial position on the cyclohexyl ring. In contrast, A16' in crenarchaeol is shifted downfield (37.80 ppm) compared to A16' in diol **1** (33.51 ppm). This strongly suggests that A16' in crenarchaeol is an equatorial position and therefore *cis* relative to the cyclopentyl substituent on A11'.

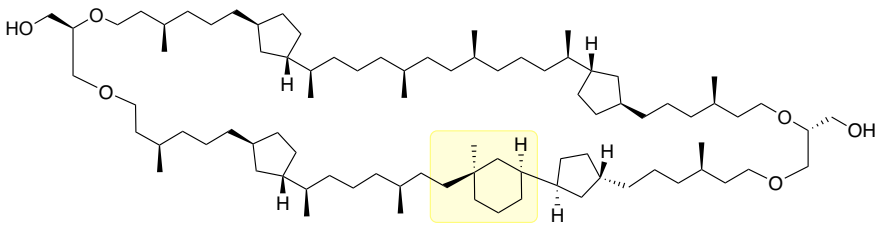

crenarchaeol

Fig. 4 *Revised structure of crenarchaeol.*

The combined analytical evidence discussed above ultimately allows us to propose beyond reasonable doubt a revised structure of crenarchaeol (Fig. 4). In this structure, the stereochemistry of A15', one of the 22 chiral centres of crenarchaeol, is inverted compared to the originally proposed structure.[8]

Currently we are working on the completion of the total synthesis of non-natural crenarchaeol containing **1** as biphytane chain in order to allow direct NMR comparison to obtain ultimate proof of structure.

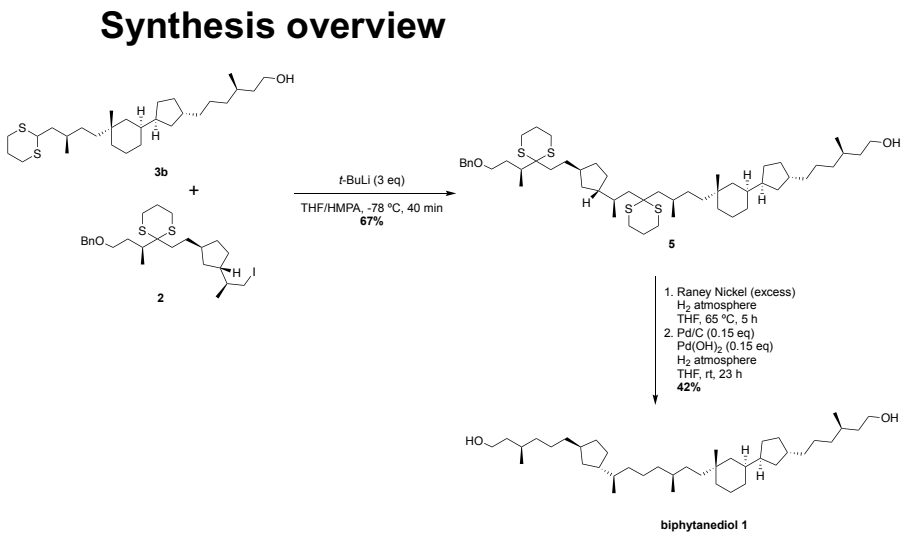

Scheme 2 *Synthetic steps in the completion of biphytanediol* ***1***

Experimental

General methods and materials

All reactions were performed using flame-dried glassware under N_2-atmosphere by Schlenk techniques, using anhydrous solvents (unless specified otherwise). Reaction temperatures refer to the temperature of the heating mantle or cooling bath.

Anhydrous solvents (MTBE, CH_2Cl_2, THF, toluene) were taken from an MBraun solvent purification system (SPS-800). Other anhydrous solvents were purchased from Sigma Aldrich or Acros Organics and used without further purification. Other reagents were purchased and used without further purification.

TLC analysis was performed on silica gel 60/Kieselguhr F_{254}, 0.25 mm (Merck). Compounds were visualized using elemental iodine followed by either Seebach stain or *p*-anis aldehyde stain.

^1H and ^{13}C NMR spectra were recorded on an Agilent 400 NMR spectrometer at 399.79 and 100.59 MHz, respectively, or on a Bruker 600 NMR spectrometer at 600.13 and 150.92 MHz, respectively using $CDCl_3$ as the solvent. Chemical shifts are reported in ppm with the solvent resonance as the internal standard (for $CDCl_3$: δ 7.26 ppm for ^1H, δ 77.16 ppm for ^{13}C). Data are reported as follows: chemical shifts (δ), multiplicity (s = singlet, d = doublet, dd = double doublet, ddd = double double doublet, ddp = double double pentet, td = triple doublet, t = triplet, q = quartet, b = broad, m = multiplet), coupling constant *J* (Hz), and integration value.

High resolution mass spectra (HRMS) were recorded on a Thermo Scientific LTQ Orbitrap XL mass spectrometer with electron spray ionization (ESI) in positive or negative mode.

Optical rotations were measured on a polarimeter (Schmidt+Haensch Polartronic MH8) with a 10 cm long cell (c given in g/100 mL) at ambient temperature (±20 °C).

Synthetic procedures

Dithiane 5

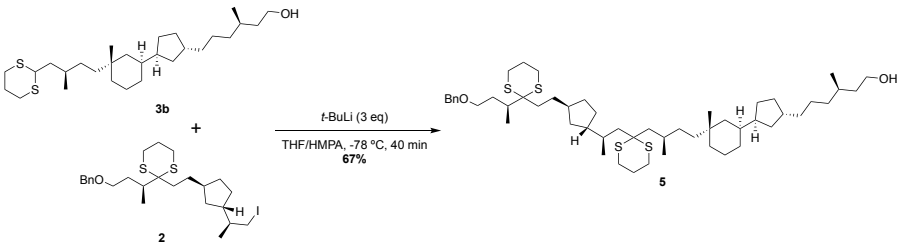

A Schlenk flask was flame-dried *in vacuo* and subjected to three cycles of evacuating and N_2 backfilling and charged with dithiane **3b** (127.5 mg, 0.272 mmol, 1.5 eq.) dissolved in dry THF (2.2 mL). Dry HMPA (0.37 mL) was added and the solution was cooled to -78 ºC. 1.7 M *t*-BuLi in hexanes (0.32 mL, 0.544 mmol, 3 eq.) was added and the reaction mixture was stirred for 10 minutes. Then, iodide **2** (100 mg, 0.183 mmol, 1 eq.) was added, dissolved in dry THF (1.5 mL) at -78 ºC. The reaction mixture was stirred for 30 min and then quenched by addition of sat. aq. NH_4Cl (15 mL). The aqueous phase was extracted with Et_2O (3 x 15 mL). The combined organic extracts were washed with brine (10 mL), dried over $MgSO_4$ and concentrated. The crude product was purified by flash chromatography (pentane/acetone 92/8) to give product **5** (109 mg, 0.123 mmol, 67% yield) as a colorless oil.

^{1}H NMR (400 MHz, Chloroform-*d*) δ 7.37 – 7.26 (m, 5H), 4.56 (d, *J* = 12.0 Hz, 1H), 4.48 (d, *J* = 12.0 Hz, 1H), 3.73 – 3.62 (m, 2H), 3.60 – 3.47 (m, 2H), 2.87 – 2.70 (m, 8H), 2.39 (dt, *J* = 14.9, 7.8 Hz, 1H), 2.15 (ddt, *J* = 11.4, 7.0, 3.5 Hz, 1H), 1.99 – 1.83 (m, 9H), 1.83 – 1.65 (m, 11H), 1.63 – 1.19 (m, 28H), 1.15 – 1.11 (m, 2H), 1.09 (d, *J* = 6.8 Hz, 4H), 1.02 (t, *J* = 6.1 Hz, 6H), 0.89 (d, *J* = 6.4 Hz, 3H), 0.80 (s, 3H), 0.75 – 0.58 (m, 2H).

^{13}C NMR (101 MHz, Chloroform-*d*) δ 138.79, 128.45, 127.69, 127.59, 72.77, 69.30, 61.38, 59.31, 55.37, 47.56, 46.02, 45.72, 43.62, 40.14, 39.78, 39.05, 39.01, 38.40, 37.54, 37.36, 36.58, 35.64, 35.33, 34.59, 34.16, 33.54, 33.41, 33.01, 32.89, 31.90, 31.79, 31.49, 31.37, 31.08, 30.72, 30.08, 29.63, 26.78, 26.07, 25.88, 25.72, 25.45, 25.23, 22.48, 22.07, 20.44, 19.80, 14.58.

HRMS (ESI+) M+H$^+$ calculated for $C_{53}H_{90}O_2S_4$: 887.5896, found: 887.5871.

Optical Rotation: $[\alpha]_D^{23}$ = -12.5° (*c* = 0.12, $CHCl_3$).

Biphytanediol 1

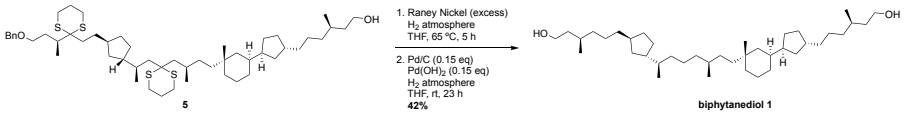

A flask was charged with Raney Nickel (2 mL, 50% dispersion in water, 10 eq. by wt., W.R. Grace and Co. Raney®2800, purchased from Sigma-Aldrich) and washed with THF (3 x 5 mL), then **5** (100.0 mg, 0.113 mmol, 1 eq.) was added, dissolved in THF (2.3 mL). H_2 was bubbled through the suspension for 2 min. The suspension was then heated to 65 °C and stirred for 5 h under H_2 atmosphere (balloon). The suspension was cooled to room temperature and the solids were removed by filtration over Celite. The filtrate was concentrated and the crude desulfurized product was dissolved in THF (2.3 mL). Pd/C (10% Pd by weight, 18.0 mg, 0.017 mmol, 0.15 eq.) and $Pd(OH)_2$ (20% Pd by weight, 11.9 mg, 0.017 mmol, 0.15 eq.) were added and H_2 was bubbled through the suspension for 5 min. The suspension was stirred at room temperature under H_2 atmosphere for 23 h. The reaction mixture was filtered over Celite and the filtrate was concentrated. The crude product was purified by flash chromatography (pentane/EtOAc 4/1) to give biphytanediol **1** (28.1 mg, 0.048 mmol, 42% yield) as colorless oil.

^{1}H NMR (600 MHz, Chloroform-*d*) δ 3.72 – 3.63 (m, 4H), 1.80 – 1.65 (m, 7H), 1.60 (dtd, *J* = 12.7, 7.2, 5.1 Hz, 2H), 1.56 – 1.52 (m, 2H), 1.49 – 1.45 (m, 4H), 1.41 – 1.33 (m, 8H), 1.31 – 1.20 (m, 18H), 1.18 – 1.02 (m, 10H), 1.01 – 0.96 (m, 2H), 0.89 (d, *J* = 6.6 Hz, 6H), 0.86 (d, *J* = 6.5 Hz, 3H), 0.84 (d, *J* = 6.6 Hz, 3H), 0.79 (s, 3H), 0.72 (qd, *J* = 12.7, 4.0 Hz, 1H), 0.67 – 0.61 (m, 1H).

^{13}C NMR (151 MHz, Chloroform-*d*) δ 61.42, 61.42, 45.73, 44.96, 43.90, 40.15, 40.14, 39.24, 39.01, 39.00, 38.45, 38.16, 37.60, 37.55, 37.52, 37.40, 37.31, 36.61, 36.16, 35.87, 33.71, 33.51, 33.39, 33.36, 32.92, 31.80, 31.41, 31.34, 30.50, 30.12, 29.65, 29.63, 26.05, 24.53, 22.10, 20.25, 19.79, 17.90.

HRMS (ESI+) M+H$^+$ calculated for $C_{40}H_{76}O_2$: 589.5918, found: 589.5900.

Optical Rotation: $[\alpha]_D^{23}$ = -4.5° (*c* = 0.11, $CHCl_3$).

Chemical derivatization

Isolation and derivatization procedures were reported previously[6, 16, 17] and done as follows:

Aliquots the GDGTs from the Bligh Dyer extract of "*Ca*. Nitrosotenius uzonensis" or **1** were subjected to ether cleavage (57% HI) described previously by Lengger *et al*.[18] The resulting primary alkyl iodides were then converted to the corresponding hydrocarbons using H_2/PtO_2.[19] The biphytanes were analyzed by GC (on-column injection) using an Agilent 7890B GC instrument as well as in splitless mode with GC–MS on an Agilent 7890A GC instrument equipped with an Agilent 5975C VL MSD detector operated at 70 eV. A CP Sil 5CB column (25 m x 0.32 mm; film thickness 0.12 µm; He carrier gas) was used to separate the biphytanes. Samples were injected at 70 °C and the GC oven was programmed to heat to 130°C (at 20 °C min^{-1}) and further heated to 320 °C (4 °C min^{-1}) temperature, which was held for 10 min.

References

1. M. Yus, C. Nájera and F. Foubelo, *Tetrahedron*, 2003, **59**, 6147-6212.
2. A. B. I. Smith and C. M. Adams, *Acc. Chem. Res.*, 2004, **37**, 365-377.
3. H.-X. Jin, Q. Zhang, H.-S. Kim, Y. Wataya, H.-H. Liu and Y. Wu, *Tetrahedron*, 2006, **62**, 7699-7711.
4. K. Ramakrishna and K. P. Kaliappan, *Org. Biomol. Chem.*, 2015, **13**, 234-240.
5. Y. Hara, T. Honda, K. Arakawa, K. Ota, K. Kamaike and H. Miyaoka, *J. Org. Chem.*, 2018, **83**, 1976-1987.
6. J. S. Sinninghe Damsté, W. I. C. Rijpstra, E. C. Hopmans, M. J. den Uijl, J. W. H. Weijers and S. Schouten, *Org. Geochem.*, 2018, **124**, 22-28.
7. S. Schouten, M. J. L. Hoefs, M. P. Koopmans, H.-J. Bosch and J. S. Sinnighe Damsté, *Org. Geochem.*, 1998, **29**, 1305-1319.
8. J. S. Sinninghe Damsté, S. Schouten, E. C. Hopmans, A. C. T. van Duin and J. A. J. Geenevasen, *J. Lipid. Res.*, 2002, **43**, 1641-1651.
9. G. W. Buchanan, *Can. J. Chem.*, 1982, **60**, 2908-2913.
10. E. Breitmaier and W. Voelter, *Carbon-13 NMR Spectroscopy: High-Resolution Methods and Applications in Organic Chemistry and Biochemistry*, VCH Verlagsgesellschaft mbH, Weinheim, Germany, 3 edn., 1987.
11. M. E. Squillacote and J. M. Neth, *Magn. Reson. Chem.*, 1987, **25**, 53-56.
12. J. Xiong, J. Wan, J. Ding, P.-P. Wang, G.-L. Ma, J. Li and J.-F. Hu, *J. Nat. Prod.*, 2017, **80**, 2874-2882.
13. E. Montenegro, B. Gabler, G. Paradies, M. Seemann and G. Helmchen, *Angew. Chem. Int. Ed.*, 2003, **42**, 2419-2421.
14. X.-L. Liu, J. S. Lipp, D. Birgel, R. E. Summons and K.-U. Hinrichs, *Org. Geochem.*, 2018, **115**, 12-23.
15. X.-L. Liu, D. A. Russell, C. Bonfio and R. E. Summons, *Org. Geochem.*, 2019, **128**, 57-62.
16. S. Schouten, E. C. Hopmans, A. Rosell-Melé, A. Pearson, P. Adam, T. Bauersachs, E. Bard, S. M. Bernasconi, T. S. Bianchi, J. J. Brocks, L. Truxal Carlson, I. S. Castañeda, S. Derenne, A. D. Selver, K. Dutta, T. Eglinton, C. Fosse, V. Galy, K. Grice, K.-U. Hinrichs, Y. Huang, A. Huguet, C. Huguet, S. Hurley, A. Ingalls, G. Jia, B. Keely, C. Knappy, M. Kondo, S. Krishnan, S. Lincoln, J. Lipp, K. Mangelsdorf, A. Martínez-García, G. Ménot, A. Mets, G. Mollenhauer, N. Ohkouchi, J. Ossebaar, M. Pagani, R. D. Pancost, E. J. Pearson, F. Peterse, G.-J. Reichart, P. Schaeffer, G. Schmitt, L. Schwark, S. R. Shah, R. W. Smith, R. H. Smittenberg, R. E. Summons, Y. Takano, H. M. Talbot, K. W. R. Taylor, R. Tarozo, M. Uchida, B. E. van Dongen, B. A. S. Van Mooy, J. Wang, C. Warren, J. W. H. Weijers, J. P. Werne, M. Woltering, S. Xie, M. Yamamoto, H. Yang, C. L. Zhang, Y. Zhang, M. Zhao and J. S. Sinnighe Damsté, *Geochem. Geophys.*, 2013, **14**, 5263-5285.
17. E. C. Hopmans, S. Schouten and J. S. Sinninghe Damsté, *Org. Geochem.*, 2016, **93**, 1-6.
18. S. K. Lengger, Y. A. Lipsewers, H. de Haas, J. S. Sinninghe Damsté and S. Schouten, *Biogeosciences*, 2014, **11**, 201-216.
19. M. Kaneko, F. Kitajima and H. Naraoka, *Org. Geochem.*, 2011, **42**, 166-172.